

EFFECTS OF TROPOSPHERIC MAPPING FUNCTIONS ON SPACE GEODETIC DATA

Sunil B. Bisnath¹, Virgílio B. Mendes,² and Richard B. Langley¹

¹Geodetic Research Laboratory, Department of Geodesy and Geomatics Engineering,
University of New Brunswick, Fredericton, New Brunswick.

²now at the Faculty of Sciences, University of Lisbon, Lisbon, Portugal.

INTRODUCTION

This report is a summary of some of the tropospheric propagation delay mapping function research performed during the past few years at the Geodetic Research Laboratory of the University of New Brunswick (UNB). The work has consisted of modelling the effect of tropospheric delay errors for geodetic and precise airborne GPS positioning. Intercomparison of mapping functions and zenith hydrostatic and wet delay models with extensive radiosonde data sets and flight data has been performed.

The research in this report covers three areas of investigation. The first is an analysis of the performance of fifteen tropospheric delay mapping functions compared against ray tracing through radiosonde data. The second is an extension of this analysis by considering how the errors from these mapping functions propagate into station coordinates. In the third investigation, a specific mapping function, the Lanyi mapping function, which has explicit tropospheric parameters, was analysed by observing the results of changing the parameters that drive the function.

TROPOSPHERIC DELAY

Radio signals travelling through the neutral atmosphere to a receiver suffer from refraction caused by electrically neutral atoms and molecules in the troposphere and stratosphere. This is commonly known as the tropospheric delay, since the bulk of the neutral atmosphere lies within the troposphere. For a signal coming from the zenith direction, assuming a spherically symmetric atmosphere, the zenith tropospheric delay is defined as:

$$d_{\text{trop}}^z = \int_{r_r}^{r_a} [n(r) - 1] dr = 10^{-6} \int_{r_r}^{r_a} N(r) dr, \quad (1)$$

where n is the refractive index, N is the refractivity, r_r is the geocentric radius of the GPS receiver antenna and r_a is the geocentric radius of the top of the neutral atmosphere. The

zenith tropospheric delay is usually divided into two components, the hydrostatic (or with some earlier models, the dry) delay and the wet delay. The hydrostatic component of the zenith delay can be modelled to a few millimetres if accurate station pressure measurements are available and the atmosphere is assumed to be in a state of hydrostatic equilibrium. The wet component, however, is highly variable both spatially and temporally and a model prediction driven by conventional surface meteorological measurements yields an accuracy of no better than 1 to 2 cm, depending on the atmospheric conditions [Langley, 1996, p. 122-3].

The zenith delay can be transformed or mapped to the delay that a signal would experience at an arbitrary elevation angle through the use of mapping functions. The mapping functions can be specified separately for the hydrostatic and the wet components according to:

$$d_{\text{trop}} = d_{\text{h}}^z \cdot m_{\text{h}}(\epsilon) + d_{\text{w}}^z \cdot m_{\text{w}}(\epsilon), \quad (2)$$

where d_{h}^z is the hydrostatic zenith delay (due mostly to dry gases), d_{w}^z is the zenith delay due to water vapour, m_{h} is the hydrostatic component mapping function, m_{w} is the wet component mapping function, and ϵ is the non-refracted elevation angle at the ground station. Note that some of the mapping functions use the *refracted* elevation angle.

ASSESSMENT OF MAPPING FUNCTIONS

Recent advances in space geodetic techniques have called for the inclusion of low elevation angle observations, for example, to reduce the correlation between the estimates of the zenith tropospheric delay corrections and the station heights, as well as to improve GPS baseline repeatability. In response, fifteen mapping functions have been tested by Mendes and Langley [1994] (see Table 1) to determine how well they operate at low elevation angles. The functions (see Table 1 for explanation of codes) BL, BE, HM, ST, and YI are based on the Hopfield [1969] model and the functions CH, DA, HE, IF, MM, and NI are based on the Marini [1972] continued fraction form. Where required, the nominal values of 6.5 K/km and 11 231 m were used for temperature lapse rate and tropopause height, respectively [Mendes and Langley, 1994]. The accuracy assessment of the mapping functions was accomplished through a comparison with ray tracing through radiosonde data.

To compute the tropospheric delay components to be used as bench mark values, radiosonde data from nine globally-distributed stations (see Table 2), representing different climatic regions, were used. The data were collected in 1992 and consist of twice-daily height profiles of pressure, temperature and relative humidity. For each station, Table 2 lists the mean and the r.m.s. about the mean of the hydrostatic and the wet components of the tropospheric delay that were computed using the refractivity constants determined by Thayer [1974] and the hydrostatic/wet formalism expressed by Davis *et al.* [1985].

Mapping Function	Year developed or introduced	ID
Baby et al.	1988	BB
Black	1978	BL
Black and Eisner	1984	BE
Chao	1972	CH
Davis et al.	1985	DA
Goad and Goodman	1974	GG
Herring	1992	HE
Moffett	1973	HM
Ifadis	1986	IF
Lanyi	1984	LA
Marini and Murray	1973	MM
Niell	1993, 1994	NI
Saastamoinen	1973	SA
Santerre	1987	ST
Yionoulis	1970	YI

Table 1. Mapping functions evaluated (from Mendes and Langley [1994]).

Station	ϕ ($^{\circ}$ N)	λ ($^{\circ}$ W)	Height (m)	no. of profiles	Hydrostatic (m)		Wet (m)	
					mean	rms	mean	rms
Guam	13.55	215.17	111	736	2.281	0.009	0.274	0.062
San Juan	18.43	66.10	3	675	2.316	0.005	0.264	0.045
Nashville	36.12	86.68	180	745	2.270	0.012	0.151	0.081
Oakland	37.73	122.20	6	740	2.313	0.010	0.115	0.035
Denver	39.75	108.53	1611	753	1.908	0.012	0.073	0.040
St. John's	47.62	52.75	140	713	2.268	0.026	0.092	0.056
Whitehorse	60.72	135.07	704	719	2.108	0.021	0.060	0.031
Kotzebue	66.87	162.63	5	687	2.299	0.025	0.056	0.042
Alert	82.50	62.33	66	720	2.282	0.022	0.032	0.023

Table 2. Location of the radiosonde stations and statistical summary of the hydrostatic and wet components of the zenith delay in metres (from Mendes and Langley [1994]).

RESULTS OF THE MAPPING FUNCTIONS ANALYSIS

The results of the assessment are summarised in Table 3. For elevation angles above 30° , virtually all mapping functions yield errors of less than 5 mm. Nearly all of the mapping functions provide subcentimetre accuracy for angles above 15° . For elevation angles below 10° , only a few of the functions were found to adequately meet the requirements currently imposed by space geodetic techniques.

The Niell, Herring and Ifadis mapping functions are quite accurate at elevation angles above 10° . The Baby, Lanyi and Saastamoinen mapping functions also perform

well. However, both the Lanyi and Davis mapping function differences with respect to ray tracing indicate some seasonal and/or latitudinal dependence. This might be caused by the use of nominal values for the tropopause height and temperature lapse rate. However, it seems likely that such nominal values will be used in space geodetic software since values of such parameters for specific sites and atmospheric conditions are generally not exactly known. This difficulty has been investigated for the Lanyi mapping function and will be discussed in the last portion of this report. The Niell, Herring, and Ifadis mapping functions are quite accurate at very low elevation angles (less than 10°) as compared to the ray tracing for the data set used. Therefore, for high-precision applications, it is recommended that the mapping functions derived by Lanyi, Herring, Ifadis or Niell be used [Mendes and Langley, 1994]. This conclusion is mirrored in the latest International Earth Rotation Service (IERS) conventions on tropospheric models for radio techniques [McCarthy, 1996]. It states that if information is available on the vertical temperature distribution in the atmosphere, the Lanyi mapping function should be used. Otherwise, one of the mapping functions derived by Ifadis, Herring or Niell should be used.

EFFECTS OF DIFFERENT TROPOSPHERIC MAPPING FUNCTIONS ON STATION COORDINATES

The previous section described how different mapping functions produce different tropospheric delay errors. But how do these errors translate into coordinate errors at observing sites? The propagation of the tropospheric delay errors into station coordinates is a function of the elevation angle, the site location, the duration of the observing session, and the domain of the carrier phase ambiguities solved for in the least-squares adjustment. To assess whether different mapping functions affect station coordinates significantly, Santerre *et al.* [1995] (at Université Laval in cooperation with UNB) propagated the tropospheric delay error from simulated GPS observations into station coordinates by solving the following set of normal equations of the least-squares adjustment:

$$d\bar{x} = (A^T P A)^{-1} (A^T P d_{\text{trop}}) = N^{-1} U, \quad (3)$$

where $d\bar{x}$ is the estimated increment to the initial value of the position vector,
 A is the design matrix of the problem,
 P is the weight matrix of the observations, and
 d_{trop} is the tropospheric delay error.

The matrix N and the vector U are accumulated epoch by epoch for a complete session. The $d\bar{x}$ vector is augmented by the carrier phase ambiguity parameters for “float solution” processing.

Station	$\epsilon(^{\circ})$	BB	BL	BE	CH	DA	GG	HE	HM	IF	LA	MM	NI	SA	ST	YI
San Juan	30	0	0.1	0.1	0.1	0.2	0.1	0.1	0.1	0.1	0.1	0.2	0.1	0.1	0.1	1.8
	15	3	1.1	0.7	1.1	1.7	0.8	0.6	1.0	0.6	0.9	1.7	0.5	1.0	0.8	1.1
	10	8	3.4	2.5	3.6	5.3	2.5	2.0	3.4	1.9	2.8	5.6	1.7	3.3	2.4	3.7
	3	93	72	59	77	63	41	36	64	35	44	104	34	72	38	73
Guam	30	0	0.2	0.1	0.2	0.3	0.1	0.1	0.1	0.1	0.1	0.2	0.1	0.1	0.1	1.2
	15	3	1.4	0.9	1.4	1.8	0.9	0.8	1.3	0.7	0.8	2.1	0.7	1.1	0.8	1.6
	10	9	4.7	3.2	4.7	5.5	2.7	2.4	4.3	2.3	2.5	6.9	2.4	3.4	2.6	5.2
	3	118	106	78	105	67	47	49	86	49	38	132	48	89	43	109
Nashville	30	0	0.3	0.1	0.3	0.6	0.3	0.2	0.3	0.1	0.3	0.5	0.1	0.2	0.2	1.4
	15	4	2.3	1.1	2.9	4.5	2.1	1.3	2.9	1.0	2.7	4.2	1.1	1.6	2.0	2.3
	10	12	7.0	3.5	9.5	14.0	6.7	4.1	9.2	3.3	8.5	13.3	3.7	5.4	6.3	7.2
	3	107	110	85	173	164	97	67	148	56	135	220	63	194	88	112
Denver	30	1	0.3	0.2	0.2	0.5	0.3	0.1	0.3	0.1	0.3	0.4	0.1	0.3	0.3	0.7
	15	4	2.4	1.3	2.2	3.4	2.6	1.3	2.2	0.9	2.7	3.0	0.9	2.4	2.5	2.4
	10	12	7.5	4.0	7.1	10.4	8.3	4.0	7.0	2.8	8.2	9.7	2.8	7.7	7.8	7.7
	3	117	106	64	125	115	122	61	113	48	111	162	50	162	112	107
Oakland	30	0	0.2	0.2	0.3	0.3	0.2	0.2	0.3	0.2	0.2	0.3	0.1	0.2	0.2	0.7
	15	4	2.1	1.9	2.2	2.4	2.1	1.7	2.2	1.6	2.0	2.6	1.1	2.1	2.0	2.1
	10	12	6.6	6.1	7.1	7.5	6.6	5.4	7.1	5.1	6.4	8.4	3.5	6.7	6.4	6.7
	3	134	105	98	117	100	103	84	111	81	97	134	60	129	99	106
St. John's	30	0	0.2	0.2	0.4	0.4	0.4	0.1	0.4	0.1	0.2	0.5	0.2	0.3	0.4	1.0
	15	3	1.7	1.8	3.1	2.9	3.0	1.2	3.2	1.1	1.8	4.5	1.4	2.7	2.9	2.1
	10	33	5.2	5.6	10.1	9.1	8.4	3.8	10.1	3.6	5.8	14.4	4.5	8.5	8.2	5.4
	3	108	90	73	177	104	88	64	159	61	92	236	76	229	83	92
Whitehorse	30	0	0.4	0.2	0.3	0.5	0.3	0.2	0.3	0.1	0.4	0.4	0.2	0.3	0.3	0.5
	15	2	3.1	1.5	2.3	3.8	2.9	1.5	2.4	1.1	3.4	3.2	1.6	2.7	2.7	3.3
	10	7	9.6	4.7	7.5	11.9	9.2	4.7	7.6	3.5	10.2	10.4	4.9	8.7	8.5	10.0
	3	67	145	57	128	135	135	74	118	59	144	168	73	167	118	146
Kotzebue	30	0	0.4	0.2	0.4	0.6	0.4	0.2	0.4	0.2	0.4	0.5	0.2	0.4	0.3	0.6
	15	2	3.4	2.1	3.3	4.6	3.2	1.5	3.3	1.3	3.7	4.2	1.7	3.1	2.9	3.8
	10	7	10.7	6.3	10.4	14.4	10.1	4.9	10.3	4.0	11.5	13.4	5.3	9.9	9.0	10.9
	3	69	159	74	174	164	146	77	161	65	172	212	79	209	121	159
Alert	30	0	0.4	0.4	0.4	0.5	0.3	0.2	0.4	0.2	0.4	0.5	0.4	0.5	0.3	0.3
	15	2	3.1	3.0	3.7	3.7	2.7	1.3	3.7	1.3	3.1	4.3	3.4	4.5	2.4	4.0
	10	5	9.7	9.3	11.5	11.6	8.7	4.1	11.5	4.0	9.9	13.4	10.6	14.3	7.5	9.9
	3	53	163	114	171	138	142	65	164	56	155	197	148	188	114	161

Table 3. Root mean square total tropospheric delay errors about the mean of the differences between the delays computed using the mapping functions and the ray trace results for various elevation angles (ϵ), in millimetres (updated from Mendes and Langley [1994]). Note that for BB, errors are rounded to the nearest millimetre.

Three sites were selected for the study: San Juan, St. John's, and Alert, and the same radiosonde data set described above was used. These sites encompass a spectrum of latitudes and meteorological conditions. For San Juan, the near-equatorial site, the satellite observations coverage is at a maximum, however, low elevation angle observations towards the north and south are not available. At St. John's, the mid-latitude site, the observations are quite sparse in the sky's northern quadrant. For Alert, the polar site, observations near the zenith are not available. The surface meteorological conditions determined from one launch of a radiosonde for each site was used, with associated tropospheric zenith delays close to the annual means. Noteworthy is the fact that the wet zenith delay contribution to the total delay is about 10% at San Juan, 4% at St. John's and 1% at Alert. Given that the Herring mapping function performed well against ray trace data [Mendes and Langley, 1994], it was used as the benchmark to compare the differences in station height computed using each mapping function.

RESULTS OF THE STATION COORDINATES ANALYSIS

Table 4 summarises the error in height due to the mapping functions as compared to the height computed using the Herring mapping function. These results are based on 24 hour simulated data series, with GPS carrier phase ambiguities considered fixed. For this data set, the Niell, Ifadis and, to a lesser extent, the Lanyi mapping functions provided the same level of performance as the Herring mapping function. As can be seen in Table 4b, 4d and 4f, the Niell, Ifadis and Lanyi functions consecutively place first, second and third, respectively, at all the sites. Note that the ranks in Table 4a, 4c and 4e are mainly driven by the values obtained at low elevation angles.

In the computation of Table 4, it was observed that some mapping functions performed better at very low elevation angles than at higher elevation angles. It was determined that this was an artifact of the models under (or over) estimating the tropospheric delay at high elevation angles and largely over (or under) estimating the tropospheric delay at lower elevation angles.

When the analysis was performed again with 12, 6 and 3 hour time series and with fixed and float solutions, the height differences varied by $\pm 10\%$. Generally, as the time spans decreased and as the ambiguities were not fixed, the variations of the results with respect to Table 4 increased.

The tropospheric delay mainly affects the station height determination; however, the effect on horizontal coordinates can also be significant (more so than for the vertical component) if the integer ambiguities are not resolved in the least-squares adjustment, the time series is short, and the elevation angle is low. Santerre *et al.* [1995] give the example of 45 minutes of simulated data at San Juan, with an elevation angle of 10° and a float solution. The difference between HM and HE is 115 mm in the east direction. The effect was reduced to 37 mm when the simulated data series was lengthened to 1.5 hours. For a

3° elevation angle and again a 45 minute simulated data series, the difference between CH and HE was 181 mm in the north direction and -197 mm in the east direction.

a) San Juan, all elevation angles		
m.f.	Total (mm)	Rank
NI	9	1
IF	17	2
LA	33	3
DA	154	4
BE	235	5

b) San Juan, all elevation angles but 3° and 5°		
m.f.	Total (mm)	Rank
NI	2	1
IF	6	2
LA	9	3
SA	18	4
CH	26	5

c) St. John's, all elevation angles		
m.f.	Total (mm)	Rank
IF	26	1
NI	32	2
DA	69	3
LA	74	4
MM	135	5

d) St. John's, all elevation angles but 3° and 5°		
m.f.	Total (mm)	Rank
NI	4	1
IF	6	2
LA	9	3
DA	10	4
SA	18	5

e) Alert, all elevation angles		
m.f.	Total (mm)	Rank
IF	80	1
NI	91	2
MM	122	3
CH	131	4
LA	139	5

f) Alert, all elevation angles but 3° and 5°		
m.f.	Total (mm)	Rank
NI	14	1
IF	16	2
LA	23	3
DA	27	4
BB	34	5

g) All sites, all elevation angles		
m.f.	Total (mm)	Rank
IF	123	1
NI	131	2
LA	245	3
DA	390	4
BE	561	5

h) All sites, all elevation angles but 3° and 5°		
m.f.	Total (mm)	Rank
NI	20	1
IF	28	2
LA	41	3
DA	74	4
SA	78	5

Table 4. Rank of the five best mapping functions for each situation, based on corresponding height differences with respect to those computed using the Herring mapping function (from Santerre *et al.* [1995]).

In relative positioning, the effect of an error in the tropospheric delay on baseline length will be less harmful if the zenith delays are similar at both sites. Generally, the shorter the baseline length and the smaller the height difference between the two sites, the more probable the zenith tropospheric delay will be similar.

It is important to remember that these results do not include the error in the evaluation of the zenith tropospheric delay.

THE EFFECTS OF CHANGING INPUT PARAMETERS IN THE LANYI MAPPING FUNCTION

The Lanyi [1984] mapping function is widely used in the processing of International GPS Service for Geodynamics (IGS) site data for various reasons, including its good performance; its ability to accept location-specific parameters of tropopause height, temperature inversion height, and temperature lapse rate; and the recommendation of its use by the IERS conventions [McCarthy, 1996]. Accordingly, the effects on the tropospheric delay of changing the values of the location-specific parameters have been studied. Measurements from the 1992 data set described above [Mendes and Langley, 1994] were again used along with additional radiosonde data compiled by the U.S. Forecast Systems Laboratory and the National Climate Data Center. The strategy used in the analysis is the same.

MIRAMAR, CA

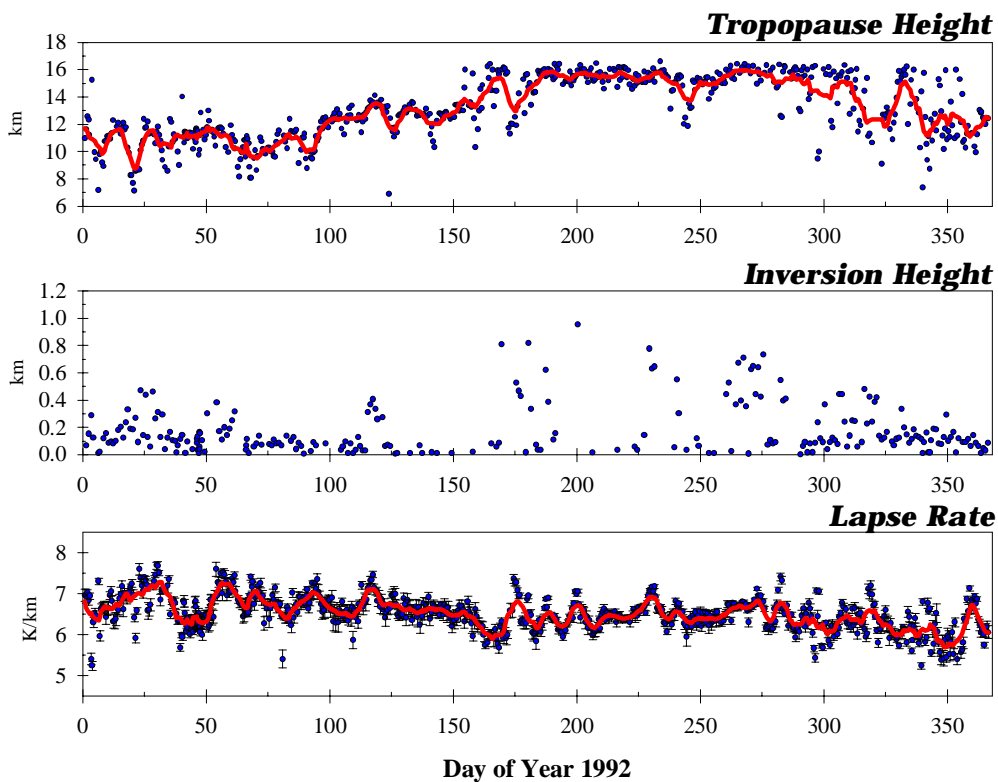


Figure 1. Variations of tropopause height, inversion height, and lapse rate through 1992 at Miramar, California. The curves represent running averages of ten points and the error bars associated with the lapse rate points are the one standard deviation limits of the lapse rate least-squares determination.

One processing strategy that is used is to drive the Lanyi function with constant parametric values. However, as illustrated in Figure 1 for Miramar, California (a site selected arbitrarily as an example), these parameters vary with time and in the case of the tropopause height, there are some seasonal variations. This will cause errors in the mapping function if mean values are used and may affect the estimation of GPS and VLBI baseline vectors.

To illustrate this point further, four different approaches to using the Lanyi mapping function were assessed at ten degrees elevation angle. The results represent the error, in metres, in the mapping function against ray tracing. The first approach uses the observed values of surface temperature, surface pressure and mean monthly values of tropopause height, inversion height and lapse rate (see Figure 2a). The second approach uses all default values recommended by Lanyi [1984] (see Figure 2b). A clear seasonal variation when the default values are used can be seen. In the third approach, the observed pressure is used, the inversion height is set to zero and the rest of the parameters are computed using the Sovers and Jacobs [1996] approach, which is an approximation to the Standard Atmospheres (see Figure 2c). Finally, the fourth approach uses the observed pressure, the mean monthly values of temperature, an inversion height of zero and default values of tropopause height (11 900 m) and lapse rate (6.1 K/km) (see Figure 2d). These latter two values are mean values determined from the analysis of 100 global radiosonde stations.

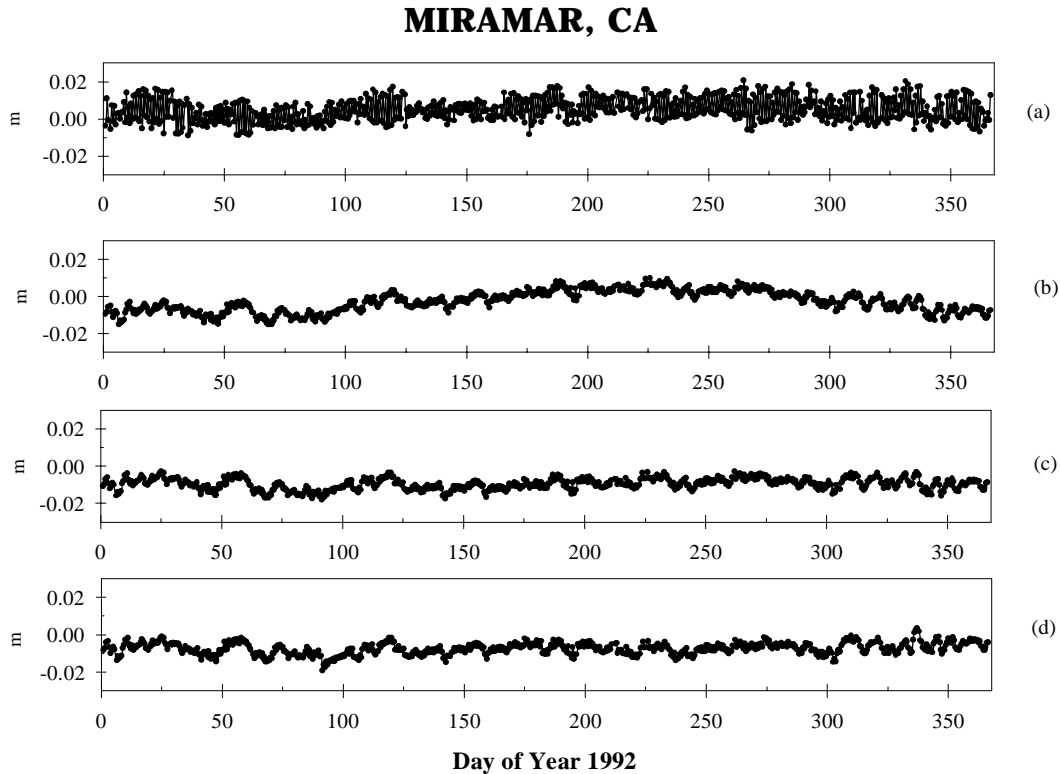


Figure 2. Total tropospheric delay error in the Lanyi mapping function, at ten degrees elevation angle, through 1992 at Miramar, California. Four different approaches to using the function (see text for details) are compared to ray tracing.

From these results it is clear that reliable tropopause determinations are required for centimetre-level tropospheric delay modelling and that seasonal variations should be taken into account (see e.g. Sovers and Jacobs [1996, p. 87] for a sensitivity analysis of the Lanyi input parameters). Also, note that a bias exists in the use of all four approaches. See Table 5 for summary statistics. There is a reduction in the scatter of the tropospheric delay error when the observed temperature is replaced with the mean monthly temperature. This illustrates the impact of meteorological data recorded at the observing site. In effect, surface temperature is not representative of the entire temperature profile through the atmosphere. However, there is no simple rule to decide which approach should be used. In the near future, these seasonal variations will be studied in more depth.

Approach	mean (mm)	r.m.s. (mm)
1	4.6	6.2
2	-3.2	5.8
3	-9.8	3.1
4	-7.7	3.2

Table 5. Mean and r.m.s. of the total tropospheric delay error in the Lanyi mapping function, at ten degrees elevation angle, through 1992 at Miramar, California. Four different approaches to using the function (see text for details) are compared to ray tracing.

For a final comparison, Figure 3 shows the total tropospheric delay errors in the Lanyi mapping function from the first approach using surface meteorological values and mean monthly values of tropopause height, inversion height and lapse rate, compared against the errors resulting from the use of the Ifadis, Herring (MMT) and Niell (NMF) mapping functions for the 1992 data set from Miramar, California. The errors represent mapping function errors in the total tropospheric delay and are for an elevation angle of ten degrees. Table 6 contains summary statistics.

Mapping function	mean (mm)	r.m.s. (mm)
Lanyi	4.6	6.2
Ifadis	-0.4	4.3
Herring	1.5	4.4
Niell	0.3	3.4

Table 6. Mean and r.m.s. of the total tropospheric delay errors in four mapping functions, at ten degrees elevation angle, through 1992 at Miramar, California, from comparisons with ray tracing.

MIRAMAR, CA

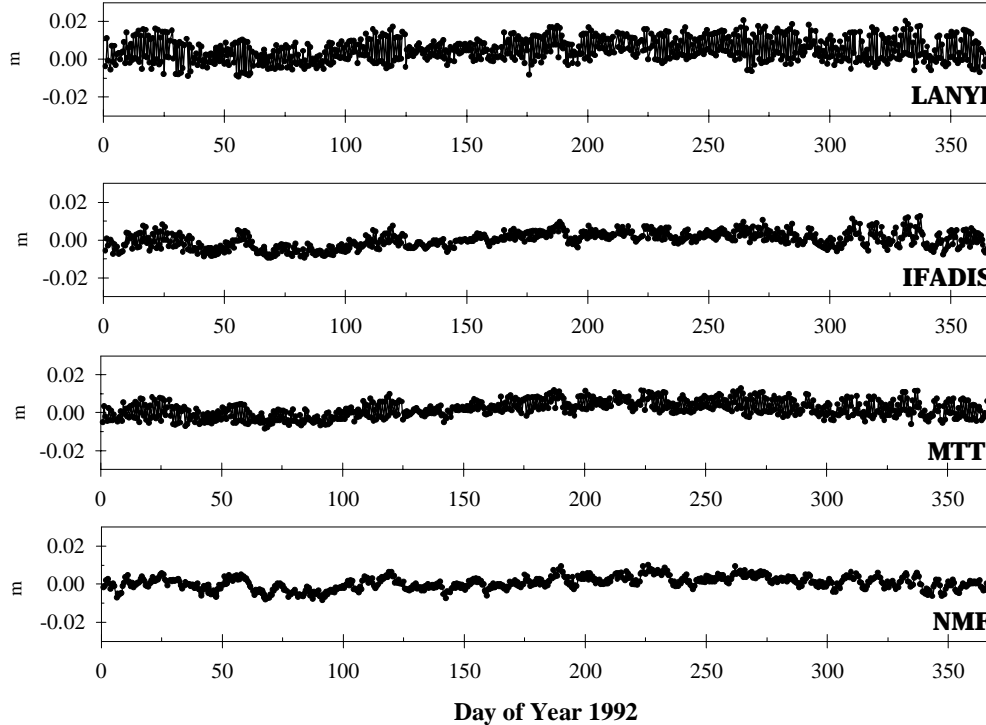


Figure 3. Total tropospheric delay errors in four mapping functions, at ten degrees elevation angle, through 1992 at Miramar, California, from comparisons with ray tracing.

SUMMARY

This report has summarised three topics of tropospheric delay research at UNB. First, an analysis of the performance of fifteen tropospheric mapping functions was performed. The second analysis investigated how the errors in the mapping functions propagate into station coordinates. And the third topic was a closer analysis of the Lanyi mapping function, which is used for processing data at many space geodesy analysis centres, and the responses obtained when the parameters that drive the function are changed.

In the first analysis, the fifteen tropospheric mapping functions were compared against tropospheric delays computed from ray tracing radiosonde data. From this analysis, it was recommended that for high precision applications, the newer mapping functions derived by Lanyi, Herring, Ifadis or Niell should be used. This conclusion was supported in the latest IERS conventions on tropospheric models for radio techniques.

In terms of their impact on position determination, when compared to the Herring mapping functions, the functions of Niell, Ifadis and Lanyi give comparable results.

Finally, for the Lanyi mapping function, it was concluded that appropriate values of the driving parameters should be carefully selected to achieve the highest accuracies. In particular, the tropopause height parameter should be carefully determined. Also, the use of surface meteorological values tends to increase the residual scatter, since these surface values are not likely to be indicative of the atmospheric profile along the signal path.

REFERENCES

Davis, J.L., T.A. Herring, I.I. Shapiro, A.E.E. Rodgers, and G. Elgered (1985). "Geodesy by radio interferometry: effects of atmospheric modeling errors on estimates of baseline length." *Radio Science*, Vol. 20, No. 6, pp. 1593-1607.

Hopfield, H.S. (1969). "Two-quartic tropospheric refractivity profiles for correcting satellite data." *Journal of Geophysical Research*, Vol. 74, No. 18, pp. 4487-4499.

Lanyi, G. (1984). "Tropospheric delay effects in radio interferometry." *Telecommunications and Data Acquisition Progress*, JPL Technical Report 42-78, Jet Propulsion Laboratory, Pasadena, Calif., U.S.A., pp. 152-159.

Langley, R.B. (1996). "Propagation of the GPS Signals," in *GPS for Geodesy*, International School, Delft, The Netherlands, 26 March - 1 April, 1995. Springer-Verlag, New York.

Marini, J.W. (1972). "Correction of satellite tracking data for an arbitrary tropospheric profile." *Radio Science*, Vol. 7, No. 2, pp. 223-231.

McCarthy, D.D. (1996). (Ed.) "Tropospheric Model." In *IERS Technical Note 21, IERS Conventions (1996)*, Central Bureau of IERS - Observatoire de Paris, July 1996, Paris.

Mendes, V.B. and R.B. Langley (1994). "A comprehensive analysis of mapping functions used in modeling tropospheric propagation delay in space geodetic data." Proceedings of KIS94, International Symposium on Kinematic Systems in Geodesy, Geomatics and Navigation, Banff, Alberta, Canada, 30 August - 2 September, 1994, pp. 87-98.

Santerre, R., I. Forgues, V.B. Mendes and R.B. Langley (1995). "Comparison of tropospheric mapping functions: their effects on station coordinates." Presented at the IUGG XXI General Assembly, 2 - 14 July, Boulder, Col., U.S.A.

Sovers, O.J. and C.S. Jacobs (1996). "Observation model and parameter partials for the JPL VLBI parameter estimation software 'MODEST' 1996." JPL Publication 83-39, Rev. 6. California Institute of Technology, Pasadena, Calif., U.S.A.

Thayer, G.D. (1974). "An improved equation for the radio refractive index of air." *Radio Science*, Vol. 9, No. 10, pp. 803-807.